J Mater Sci (2007) 42:7375–7380
DOI 10.1007/s10853-006-1310-2

Non-destructive analysis of silver selenide films obtained by Pulsed Laser Deposition (PLD) with Micro-XRF

Rainer Dargel · Mohamed Azeroual · Boris Mogwitz · Juergen Janek · Carla Vogt

Received: 24 August 2006 / Accepted: 21 November 2006 / Published online: 15 May 2007

Abstract Thin films of silver selenide with varying composition have been deposited on magnesium oxide substrates with pulsed laser deposition and were investigated via micro-XRF. A calibration procedure was designed to determine the absolute thicknesses of the films. The lateral homogeneity was investigated by elemental mapping, thus delivering information about the deposition process. Wet chemical analysis was performed on the dissolved layers with ICP-OES and ICP-MS to determine the stoichiometry of the Ag_xSe_y. The results suggest a correlation between the composition of the layers and their thicknesses by showing a silver enrichment for thinner layers.

Introduction

Thin layer technologies enclose a large potential of current and future applications. The usage of films instead of bulk material often leads to drastically reduced costs by using cheap substrates while keeping the properties of the coating material. They are being used in such diverse areas as corrosion protection, decoration, microelectronics, superconductors etc [1]. Because of the broad range of substrates and application fields, numerous procedures for the production of thin layers are presently used and developed, like pulsed laser deposition (PLD), chemical vapour deposition (CVD) and Galvanic coating processes [2]. The quality of the films depends in particular on their thickness, microstructure and chemical homogeneity. To control these parameters miscellaneous techniques like x-ray diffractometry (XRD), scanning electron microscopy (SEM), transmission electron microscopy (TEM), rutherford backscattering spectroscopy (RBS), secondary ion mass spectrometry (SIMS), or laser ablation-ICP-mass spectrometry (LA-ICP-MS) are being used [3, 4]. X-ray fluorescence has been a standard technique for the determination of layer properties for several decades now [5], because of its non-destructive nature, its speed and precision. The mediocre lateral resolution of a few square millimetres, which hampered its application in modern micro technology, has been significantly improved by the development of the micro-XRF, thus opening new fields of application [6].

Overstoichiometric Silver selenide is due to its large and linear magnetoresistance [7] a very promising candidate for the development of new magnetoresistive sensors, as Husmann et al. [8] showed by using $Ag_{2+\delta}Se$ as a Megagauss sensoring material.

In this work silver selenide layers of different thicknesses were investigated regarding thickness, homogeneity and stoichiometry. Micro-XRF was used to develop a calibration procedure to quantify film thicknesses by using the fluorescence signal. Distribution mappings were performed to investigate the homogeneity of the films in order to gain information about the layer-quality and the deposition process. The composition of the silver selenide was

R. Dargel · M. Azeroual · C. Vogt (✉)
Department of Analytical Chemistry, Institute for Inorganic Chemistry, University of Hannover, Callinstr. 9, 30167 Hannover, Germany
e-mail: C.Vogt@acc.uni-hannover.de

R. Dargel
e-mail: Rainer.Dargel@acc.uni-hannover.de

B. Mogwitz · J. Janek
Institute of Physical Chemistry, University of Giessen, Heinrich-Buff-Ring 58, 35392 Giessen, Germany

determined by dissolution of the layer and subsequent analysis with inductively coupled plasma optical emission spectrometry (ICP-OES) and mass spectrometry (ICP-MS).

Applications and preparation of silver selenide films

There are a number of reports on an unusually large linear magnetoresistance (MR) effect in silver-rich α-silver selenide ($Ag_{2+\delta}Se$) samples with compositions in the range of $\delta = 5 \cdot 10^{-5}$ up to $\delta = 0.33$ [9, 10]. For closer investigations the (magneto) size effect of thin silver selenide films within a wide range of thicknesses and with a defined stoichiometry was investigated. Different preparation methods such as physical vapour deposition (PVD) of Ag_2Se, reaction of separately deposited selenium on top of a silver film (high-temperature successive deposition, HTSD) and pulsed laser deposition (PLD) [11] have been evaluated. It was found that PLD is the best approach to produce homogeneous films in the desired thickness from about 10 nm up to several μm. For the preparation of the silver selenide films Ag_2Se targets were used. The silver selenide has been prepared by co-melting of stoichiometric amounts of silver and selenium (both Chempur 99.999 % purity) in an evacuated quartz ampoule at a temperature of approximately 1200 K for 24 h. The melt was cooled to room temperature (in about 15 minutes), the resulting polycrystal was cut in circular pellets with a diameter of about 15 mm and a thickness of 3 mm. Its homogeneity was ensured by XRF distribution mappings.

The PLD setup consists of a Kr-F excimer laser (Compex 201 Lambda-Physik, $\lambda = 248$ nm) and a standard high vacuum chamber. We found that a pulse energy of 200 mJ and a repetition rate of 10 Hz leads to Ag_2Se films with sufficient and reproducible quality. The films were deposited on cleaved magnesium oxide substrates (10 mm × 10 mm) at a temperature of 390 K with an argon background pressure of 20 Pa. During the deposition process the substrate was held at a temperature of 393 K, below the phase transition temperature ($T = 406$ K) of silver selenide, and then slowly cooled down to room temperature.

In the last step the films were annealed for 2 h at a temperature of 323 K in vacuum (about 10 mbar). Details of the PLD process can be found elsewhere [12].

For this study 26 samples with silver selenide layers on magnesium oxide substrates were prepared and divided into two series. The first series, with layer thicknesses ranging from 27 to 1800 nm, served to establish a calibration routine for the XRF measurements. The second sample series, ranging from 175 to 1075 nm, was used to investigate the lateral homogeneity of the layers and, after dissolution of the layers, to investigate the stoichiometry by wet chemical analysis.

Micro x-ray fluorescence analysis (micro-XRF) and its use in thickness measurements

X-ray fluorescence analysis is a standard analytical method in numerous fields of application in science, industry and quality control [13]. The advantages of x-ray fluorescence lie in its non-destructive nature, the speed and precision of the measurements and the comparatively easy sample preparation. However, its use as an analytical tool is in many areas like microelectronics severely hampered due to its insufficient lateral resolution in the range of mm^2 to cm^2. Recent technological advancements led to the development of x-ray optics that use total reflection to focus x-rays to spot sizes in the range of tens of micrometers. The principle of micro-XRF is given elsewhere [6, 14]. The potential of the micro-XRF for the quality control of layered structures with high lateral resolution was shown in earlier studies [14, 15]. The determination of layer thickness by XRF is based on the relation between the fluorescence intensity and the thickness of the layer. In the so called absorption mode the intensity of the substrate signal is measured as it is weakened by the layer material. This relation is approximately given by the well-known Lambert law (1):

$$I = I_0 \cdot e^{-\mu d} \tag{1}$$

with I and I_0 being the intensity of the fluorescence radiation of the substrate, the layer thickness d and the extinction coefficient μ, a material constant [5]. For small values of $\mu \cdot d$ the exponential expression evolves into a linear correlation. After application of Taylor series expansions for the exponential terms [16] the simplified Eq. 2 is obtained:

$$I \approx I_0 - (\mu \cdot I_0) \cdot d \tag{2}$$

The expression for the emission mode, i.e. the measurement of the intensity of the elements in the layer, is not suitable for routine calibration procedures due to its complexity and is discussed elsewhere [17].

Experimental

An energy dispersive micro x-ray fluorescence spectrometer (Eagle μProbe II) with a polycapillary optic of 50 μm spotsize and a rhodium anode was used for the fluorescence measurements. All measurements were done at 40 kV and 1 mA at 6 μs amplification time in a vacuum atmosphere. The Mg-K, Ag-L and Se-K lines were evaluated, with α-Energies at 1.253 keV, 2.984 keV and 9.874 keV, respectively. The equipment for inductively-coupled-plasma

mass-spectrometry (ICP-MS) was a Thermo X7 ICP-MS, for inductively-coupled-plasma optical emission spectrometry (ICP-OES) a Spectroflame Modula ICP-OES was used.

For the film thickness calibration XRF measurements were taken at five spots located in the corners and the centre of each sample surface, which were approximately 0.8 cm long and 0.8 cm wide. The arithmetic means of the measured intensities were plotted against the film thicknesses, which have been obtained by cleaving of the samples and SEM-measurements of the cross-sections. For the element distribution measurements 200×200 spots were measured with an overlap of about 10 µm, leading to mapping areas of 810 µm × 810 µm. The fluorescence signals were transferred into absolute thicknesses by the corresponding calibration curve. For the investigation of the stoichiometry by OES and MS the silver selenide layers were submerged in 5 g 68% concentrated nitric acid and dissolved in an ultrasonic bath for 3 h at 300 K. The clear solution was diluted with 25 g of high-purity water. The concentrations after this dilution were approximately 1–11 ppm for Se and 3–35 ppm for Ag. For the ICP-OES analysis these samples were measured without further dilution. For the ICP-MS analysis the same sample solutions were diluted 1:1000, except the sample with the film thickness of 27 nm, which was diluted 1:100.

Results and discussion

In Figs. 1 and 2 the average X-ray intensities for the five-point-measurements of the samples are plotted against the layer thickness. The corresponding standard deviations are given as error bars.

It was found that both in emission mode as in absorption mode the response of the thinnest films was linear, with

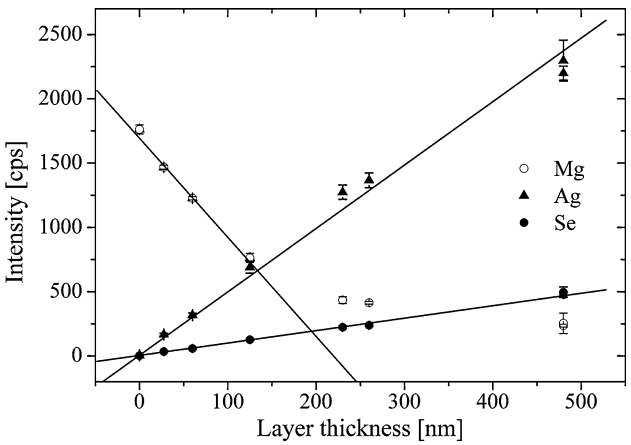

Fig. 1 Micro-XRF intensity calibration curves for silver selenide layers with $d < 200$ nm for Mg and $d < 500$ nm for Ag and Se

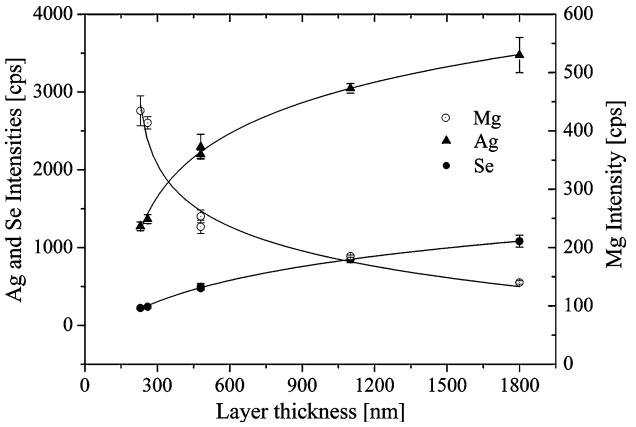

Fig. 2 Micro-XRF intensity calibration curves for silver selenide layers with $d > 200$ nm

good correlation coefficients for the fitting curves (Ag-L: $R^2 = 0.992$; Se–K: $R^2 = 0.997$ and Mg–K: $R^2 = 0.992$). This agrees with equation 2 for the absorption signal. The linear range ends for Mg at 125 nm, while it extends for Ag and Se up to 500 nm. For thicker samples the expected non-linear behaviour can be observed in Fig. 2, with an asymptotic progression towards a saturation thickness. The curvatures of the calibration lines for thicker layers are due to secondary excitation and absorption effects, which are negligible for the thinner films. The fairly low standard deviations indicate rather homogeneous layer thicknesses. The correlation coefficients are close to unity, indicating that both the emission and absorption curves can be exploited for a reliable quantitative thickness determination. It can be estimated from the curves in Fig. 1 that the lowest detectable thicknesses are a few nanometres. The slope of the linear Ag curve is steeper than the Se curve, so the layer analysis with the Ag signal is more sensitive.

In Figs. 3–6 the selenium and silver distributions for two samples with film thicknesses of 60 nm and 480 nm are shown.

Figure 3 shows a uniform distribution of selenium for the 60 nm-sample while an enrichment of silver can be observed in Fig. 4 in the bottom left corner. In contrast to this the 480 nm sample shows a less homogeneous distribution for selenium in Fig. 5 and a lower amount of silver in Fig. 6.

The standard deviations for silver are generally higher than for selenium, which hints that the selenium is more homogeneously distributed than silver. This agrees with the mappings. This might be explained by the higher volatility of selenium which is able to establish a uniform atmosphere in the deposition chamber, in contrast to the silver, which is deposited rapidly in the vicinity of the Ag_2Se-Target. XRF-measurements on an aluminium foil deposited in the vacuum pump confirmed this assumption by showing

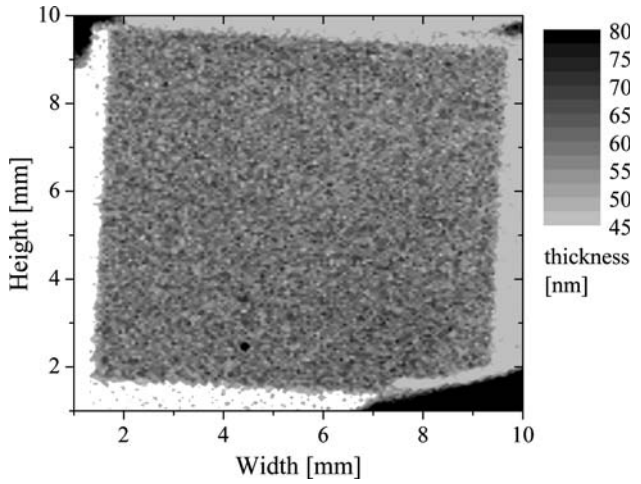

Fig. 3 Distribution of layer thicknesses on the basis of the selenium signal with layer thickness of approximately 60 nm

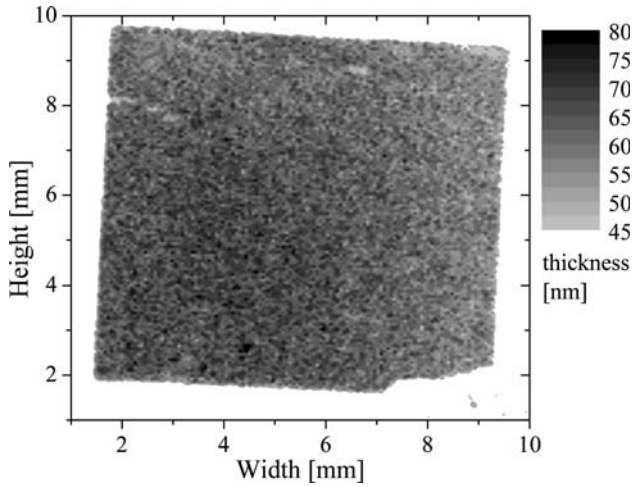

Fig. 4 Distribution of layer thicknesses on the basis of the silver signal with layer thickness of approximately 60 nm

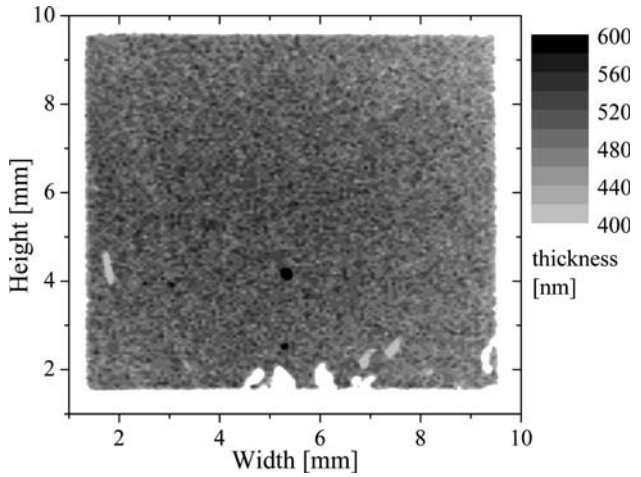

Fig. 5 Distribution of layer thicknesses on the basis of the selenium signal with layer thickness of approximately 480 nm

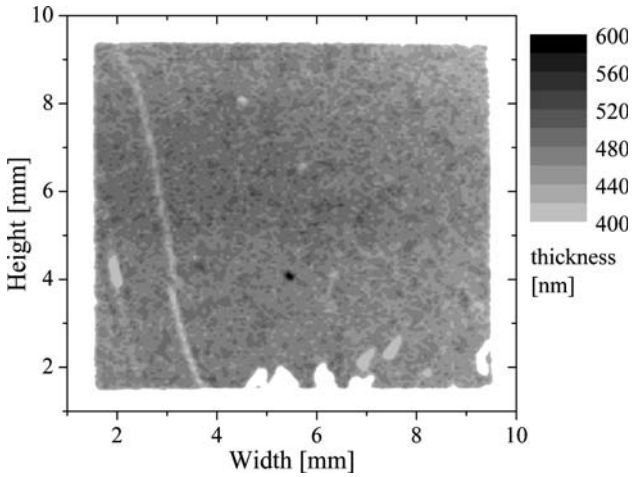

Fig. 6 Distribution of layer thicknesses on the basis of the silver signal with layer thickness of approximately 480 nm

a pure selenium layer on the foil. The presence of the proposed concentration profiles will in future be checked by depth profiling of samples with thick layers via glow-discharge optical emission spectroscopy.

The silver selenide is usually deposited in a circular pattern (Fig. 7), as was expected from the geometry of the deposition setup. In three cases however we observed a streak like structure, of which one is shown in Fig. 8.

The origin of the streaks has not yet been definitely clarified, as several explanations are possible. We can rule out the possibility of a degradation of the target, as the subsequently produced layer showed a circular pattern. As the arrangement for the heating of the layers is the same for each sample, the pattern does not reproduce an image of the heating coil. The most probable explanation is that the

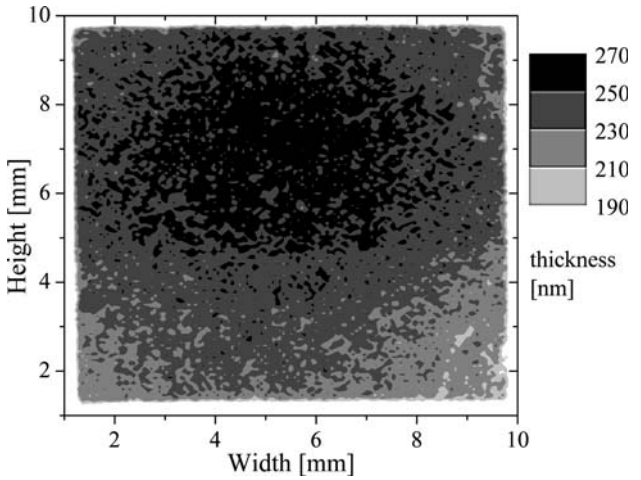

Fig. 7 Distribution of layer thickness on the basis of the silver signal for the sample with a layer thickness of approximately 230 nm (circular structure)

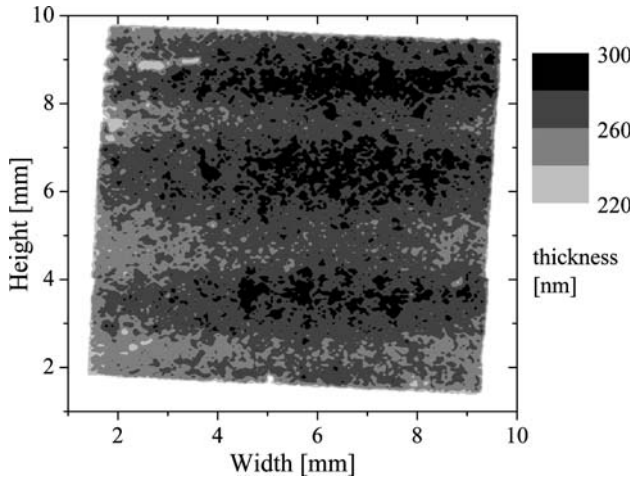

Fig. 8 Distribution of layer thickness on the basis of the Ag signal for the sample with a layer thickness of approximately 260 nm (streak-like structure)

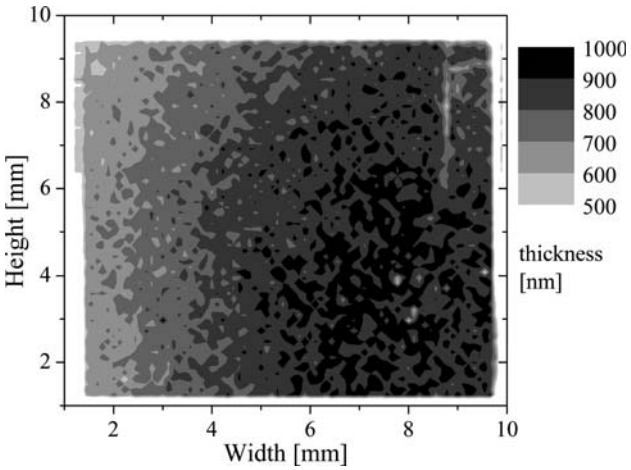

Fig. 10 Distribution of layer thickness on the basis of the silver signal for the laser sputtering on the right side of the PLD target

superposition of the rotation movement of the Ag_2Se-target and the lateral movement of the laser beam on the target led to interferences. Measurements of layers with varying PLD conditions will be carried out in the future to verify this assumption. What we have observed is an influence of the position where the PLD target is being hit by the laser. Two samples have been prepared with two different laser input positions, left and right of the centre of the target. The corresponding distribution patterns given in Figs. 9 and 10 show a migration of the maxima from the bottom left corner to the left side.

The wet chemical analysis of the layers showed a persistent excess of silver relative to the stoichiometric formula Ag_2Se. The ratio of the stoichiometry coefficients is plotted against the layer thickness in Fig. 11.

The results differ in their absolute value due to the difficult quantification with ICP-MS. On the mass-to-charge-ratios of the selenium isotopes are prominent interferences, for example by the formation of Argon–Argon dimers. The qualitative trend however agrees with the OES-measurements. The amount of silver decreases with increasing layer thickness, which agrees with the trend observed in the distribution mappings in Figs. 4 and 6. This might also be explained by the higher volatility of the selenium. While the less volatile silver is instantly deposited on the substrate the selenium spreads into the chamber and is partially sucked into the vacuum pump. For the thicker samples the deposition process lasts longer, which gives the selenium enough time to establish an equilibrium concentration within the gas phase, offering enough material to be incorporated into the layer. Thus a concentration profile within the layers should be established, with

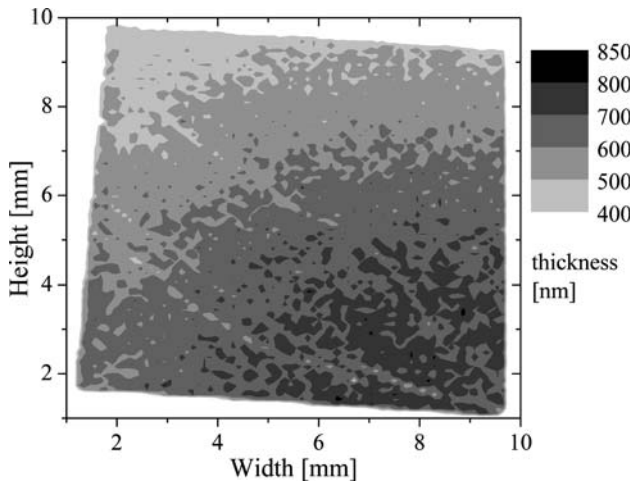

Fig. 9 Distribution of layer thickness on the basis of the silver signal for the laser sputtering on the left side of the PLD target

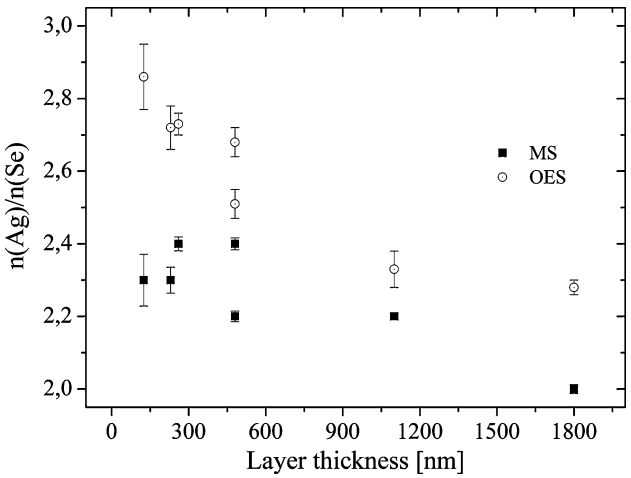

Fig. 11 Variation of stoichiometry as a function of the layer thickness measured by ICP-MS and ICP-OES

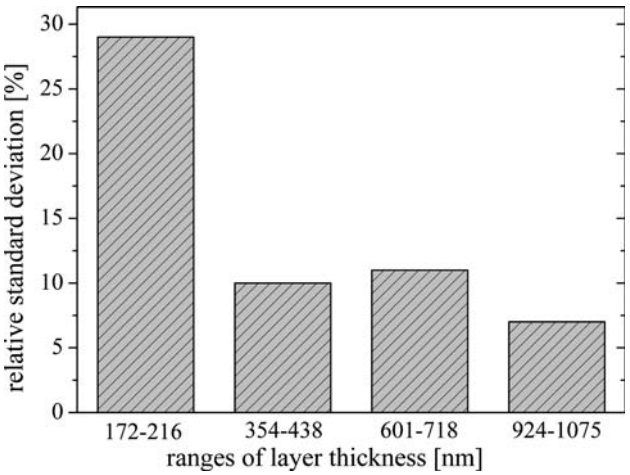

Fig. 12 Investigation of the reproducibility of the coating process determined via the stoichiometry of the layer

a decreasing silver concentration from the substrate to the surface. The results for the thinnest layers are questionable as the total masses of the separated layers were almost too low to handle (<1 mg). The concentrations of these samples as determined by ICP-OES were below the limits of detection, being 0.8 ppm for silver and 1.6 ppm for selenium, respectively.

To investigate the reproducibility of the composition of the films four sample-sets with different layer thickness ranges and with four individual samples each were examined. The compositions determined for each sample of the different sets have been averaged and the corresponding relative standard deviations were compared (Fig. 12).

With lower film thicknesses a significantly higher variation in the stoichiometry of the produced layers was observed. These higher variations of the Ag/Se molar ratio are probably caused by fluctuations of the composition (selenium partial pressure) of the emerging gas phase during the deposition, which are more significant at short deposition times.

Summary

Silver selenide films on magnesium oxide substrates have been investigated with micro-XRF and wet chemical analysis. Micro-XRF proved to be suitable for the quantitative determination of layer thicknesses in the region of 2–2000 nanometres when appropriate calibration standards are available. By means of micro-XRF Ag_xSe_y films with thicknesses as low as 5 nm or 2 nm using the Se or the Ag signal, respectively, can be determined.

With a lateral resolution of tens of micrometers the distribution of the layer components could be evaluated, thus providing information about the quality of the deposition process. An influence of the position of the plasma plume on the deposition pattern was observed. For the determination of the composition of the films spectroscopic methods were applicable, when the mass of the films was sufficiently large to handle the dissolution process. In this work the minimal mass of a film that could be analysed by ICP-OES was approximately 24 μg for Ag and 48 μg for Se, using 30 ml solution of the dissolved layers.

Further experiments will include the variation of the deposition parameters, especially the point of laser impact as well as the synchronization of the lateral laser movement and the rotation of the target. The proposed concentration profile will be checked by measuring cross-sections of thick samples via Micro-PIXE, which provides high sensitivity with spot-sizes of a few hundred nanometres. Besides that, depth-profiling measurements with glow-discharge-OES will be performed.

References

1. Kienel G (1993) Vakuumbeschichtung Anwendungen Teil 1. VDI Verlag GmbH, Duesseldorf
2. Wasa K, Kitabatake M, Adachi H (2004) Thin film materials technology—Sputtering of compound materials
3. Bubert H, Jenett H (2002) Surface and thin film analysis. VCH, Weinheim
4. Lifshin E (1994) Characterization of materials, Vol. 2. Wiley-VCH, Weinheim
5. Cammann K (2000) Instrumentelle analytische Chemie. Spektrum Akademischer Verlag GmbH, Heidelberg, Berlin
6. Janssens KHA, Adams FCV, Rindby A (eds) (2000) Microscopic X ray fluorescence analysis. Wiley, New York
7. Xu R, Husmann A, Rosenbaum TF, Saboungi ML, Enderby JE, Littlewood PB (1997) Nature 390:57
8. Husmann A, Betts JB, Boebinger GS, Migliori A, Rosenbaum TF, Saboungi ML (2002) Nature 417:421
9. Beck G, Janek J (2001) Physica B 308–310:1086
10. Xu R, Husmann Y, Rosenbaum TF, Saboungi ML, Enderbya JE, Littlewoo PB (1997) Nature 57
11. Kreutzbruck Mv, Mogwitz B, Gruhl F, Kienle L, Korte C, Janek J (2005) Appl Phys Lett 86:072102 1–3
12. Chrisey DB, Hubler GK (1994) Pulsed laser deposition of thin films. Wiley and Sons, New York
13. Hahn-Weinheimer P, Hirner A, Weber-Diefenbach K (1995) Roentgenfluoreszenzanalytische Methoden. Vieweg Verlag, Wiesbaden
14. Vogt C, Dargel R, Täschner C, Bartsch K (2004) GIT-Laborfachzeitschrift 683–685
15. Vogt C, Dargel R, (2005) Appl Surf Sci 252:53
16. Walter W (1990) Analysis 2. Springer Verlag, Berlin
17. Haar LMvd, Sommer C, Stoop MGM (2004) Thin Solid Films 450:90